KINETIC MONTE CARLO SIMULATION OF CATION DIFFUSION IN LOW-K CERAMICS.

Brian Good, Materials and Structures Division, NASA Glenn Research Center
Cleveland, OH, USA

ABSTRACT

Low thermal conductivity (low-K) ceramic materials are of interest to the aerospace community for use as the thermal barrier component of coating systems for turbine engine components. In particular, zirconia-based materials exhibit both low thermal conductivity and structural stability at high temperature, making them suitable for such applications. Because creep is one of the potential failure modes, and because diffusion is a mechanism by which creep takes place, we have performed computer simulations of cation diffusion in a variety of zirconia-based low-K materials. The kinetic Monte Carlo simulation method is an alternative to the more widely known molecular dynamics (MD) method. It is designed to study "infrequent-event" processes, such as diffusion, for which MD simulation can be highly inefficient. We describe the results of kinetic Monte Carlo computer simulations of cation diffusion in several zirconia-based materials, specifically, zirconia doped with Y, Gd , Nb and Yb. Diffusion paths are identified, and migration energy barriers are obtained from density functional calculations and from the literature. We present results on the temperature dependence of the diffusivity, and on the effects of the presence of oxygen vacancies in cation diffusion barrier complexes as well.

INTRODUCTION

The high melting point of zirconia makes the material useful for high-temperature applications. However, zirconia undergoes two phase transitions between room temperature and the melting point; it exists in a monoclinic structure below about 1100°C, a tetragonal structure between 1100°C and 2300°C, and a cubic structure between 2300°C and the melting point.[1] While this would seem to render the material unsuitable for such applications, the addition of substitutional aliovalent cation dopants such as Y^{3+} can stabilize the tetragonal and cubic phases. The high-temperature cubic phase can be fully stabilized, retaining the cubic structure from room temperature to the melting point. Fully stabilized zirconia exists in a cubic fluorite structure in which the cations are located on a face-centered cubic sublattice, with the oxygen ions located on a simple cubic sublattice whose lattice constant is one-half that of the cation sublattice.

Yttria-stabilized zirconia (YSZ) exhibits both thermal stability and low thermal conductivity, making it suitable for use as a component of coating systems for aerospace applications, for example, the thermal protection component of a coating system for turbine engine components. It exhibits oxygen and cation diffusive ionic conduction, both of which are generally considered to occur via the hopping of ions to nearest-neighbor vacancies on the appropriate sublattice. However, the detailed mechanisms of the two cases are somewhat different, resulting in very different dependences of the diffusivity on the cation dopant concentration.

The high ionic oxygen conductivity makes YSZ-based materials of interest for use as oxygen sensors, or as solid electrolytes for fuel cells. However, in the case of YSZ the oxygen diffusivity does not increase monotonically with Y^{3+} concentration; it increases at low concentrations, but reaches a maximum between 8 and 15 mol % Y_2O_3, and decreases at higher concentrations.[2]

When oxygen ions move diffusively on the oxygen sublattice, they pass through a two-cation barrier complex, the composition of which determines the migration energy barrier. Substitutional doping by cations whose ionic charge is smaller than that of Zr^{4+} results in the formation of additional oxygen vacancies beyond the intrinsic concentration, as needed to maintain electrical neutrality. On the other hand, increasing the cation dopant concentration also increases the fraction of diffusion barrier complexes that contain one or two dopant ions, and these energy barriers will be different from the energies of barriers consisting of two Zr^{4+} cations; for barriers containing one or two Y^{3+} cations, the barrier energies are larger than that of a two- Zr^{4+} barrier.

The behavior of the oxygen diffusivity as a function of dopant concentration may be understood as a competition between the two effects described above. As the Y concentration increases, the number of oxygen vacancies available as target sites for diffusive hops increases, increasing the diffusivity. However, increasing the Y concentration also increases the number of higher-energy ZrY and YY complexes, which tends to reduce the diffusivity.[3,4]

Cation bulk diffusion in these materials is several orders of magnitude slower than oxygen diffusion.[5] Bulk diffusion takes place via diffusive hopping of cations among vacancies on the cation sublattice, with the cations passing through a barrier complex consisting of two oxygen atoms. In contrast to oxygen diffusion, Y^{3+} doping has no strong direct effect on the concentration of vacancy sites on the cation sublattice, and the number of target vacancy sites remains at the intrinsic value. However, because cation doping increases the concentration of vacancies on the oxygen sublattice, there will be a change in the fraction of barrier complexes containing fewer than two oxygen atoms, which may have an indirect effect on the cation diffusivity.

Cation diffusion is a mechanism by which creep takes place, which can affect the mechanical integrity and phase stability of the material, and the utility of alternate dopants will be limited if their inclusion substantially increases cation diffusion. Zhu and Miller investigated the thermal conductivity of YSZ with additional dopants, with the goal of developing reduced-k materials.[6] They found that, compared with a YSZ 4.55 mol% Y_2O_3 baseline concentration, both YSZ-Nd-Yb and YSZ-Gd-Yb showed a reduced thermal conductivity at a temperature of 1316C, in some cases showing a reduction in thermal conductivity by more than a factor of two. The best YSZ-Nd-Yb samples showed a thermal conductivity slightly lower than that of the best YSZ-Gd-Yb. The thermal conductivity was found to increase with thermal cycling time. The increase was largest for YSZ, with smaller increases for YSZ-Nd-Yb and YSZ-Gd-Yb. Other aspects of the thermal cycling results were ambiguous. For plasma-sprayed coatings, YSZ-Nd-Yb showed a lower cycles-to-failure than YSZ-Gd-Yb. However, for electron-beam

physical-vapor-deposited coatings, the trend was reversed. In both cases, there was considerable scatter in the data

In view of the range of potential applications, considerable experimental and theoretical effort has gone into understanding the microstructure and phase behavior of YSZ. Of interest here, computer simulations using a variety of techniques have been performed. The tetragonal-to-cubic phase transition in YSZ has been investigated by Schelling et al. using molecular dynamics simulation with a Coulomb+Buckingham potential.[7] They correctly predicted the experimentally observed stabilization due to the doping of zirconia with yttria. Fabris et al. have carried out similar work using empirical self-consistent tight-binding molecular dynamics in conjunction with a Landau approach, to describe the thermodynamics of the transtion.[8] Fevre et al. have investigated the microstructure of YSZ experimentally via neutron scattering and theoretically via Monte Carlo and molecular dynamics simulation, also using a Coulomb+Buckingham potential.[9] Fevre et al. have also investigated the thermal conductivity of YSZ using nonequilibrum molecular dynamics, finding that the conductivity increases with yttria concentration for yttria-rich compositions and for temperatures below 800K, but decreases with concentration at high temperatures for all concentrations.[10]

A number of computational studies of oxygen diffusion in YSZ have been performed using a variety of techniques. Kahn et al. performed molecular dynamics simulations of oxygen diffusion in YSZ doped with a variety of dopants.[11] In particular, they considered the detailed bonding of oxygen vacancies to various dopant cations, including rare earths. They found that for Y^{3+}, La^{3+}, Nd^{3+} and Gd^{3+}, the binding of a dopant ion to a nearest neighbor oxygen vacancy was not favored energetically, though binding to a next nearest neighbor vacancy was favored. Other MD studies of oxygen diffusion have been performed by Perumal[12] and Shimojo.[13] Okazaki et al. investigated the effect of the ordering of Y dopants in YSZ, and showed that the oxygen diffusivity is enhanced compared to YSZ containing randomly distributed Y dopants.[14] Krishnamurthy et al. have performed kinetic Monte Carlo (kMC) simulations of oxygen diffusion in YSZ[3] and lanthanide-doped YSZ[4], and produced diffusivities in reasonable agreement with experiment.

Because cation diffusion in YSZ is orders of magnitude slower than oxygen diffusion, it is less amenable to study via molecular dynamics simulation, especially at lower temperatures. Some theoretical work does exist, however. Kilo et al. have analyzed Zr diffusion from creep data, dislocation loop shrinkage data, and Zr tracer diffusion data to identify the defects responsible for cation diffusion, and show that diffusion involving single cation vacancies as the most likely mechanism.[15] However, they note that the measurement of activation energies remains problematic; the relative ordering of the energies for Zr and Y diffusion are not consistent among various studies.

Kilo et al. performed simulations of cation diffusion in YSZ (as well as doped lanthanum gallates), using NPT molecular dynamics and a Buckingham+Coulomb potential.[16] They considered the hopping of cations via vacancy sites, introduced in the form of Schottky defects, at a mole fraction of 0.004, for yttria mole fractions of 0.11,

0.19 and 0.31. They found that cation diffusion is controlled by cation vacancies; interstitial diffusion is not significant. They also found that the diffusion coefficients for Y and Zr are significantly different, with Y diffusion 3-5 times faster than Zr diffusion. They reported calculated enthalpies, for YSZ with a yttria concentration of 11 mol %, of 4.8eV (Y) and 4.7eV (Zr). These vary in both magnitude and ordering from experimental results from Kilo et al.[15], who reported 4.2eV (Y) and 4.6eV (Zr). Their molecular dynamics results also showed that cation diffusivities were independent of Y_2O_3 concentration, or slightly increasing with increasing Y_2O_3 concentration, in contrast with the results of Fevre.[9,10]

Kilo et al. performed tracer diffusion studies of Y, Ca and Zr in yttria- and calcia-stabilized zirconia, and found a correlation of cation diffusivity with the ionic radius of the diffusing ion.[5] Zr and Y bulk diffusivities were maximized for a stabilizer content of 10-11 mol %. Activation enthalpies were found to be 4.2eV for Y and 4.5eV for Zr. In addition, the experimentally measured prefactor was of the same order for the two materials, 0.041 for Zr^{4+}, and 0.024 for Y^{3+}, suggesting that the vibrational frequencies for the two ions are not very different. However, for other cations, the prefactors differed from these by up the three orders of magnitude. The yttrium diffusivity decreased with increasing yttrium concentration, in contrast to the behavior observed in molecular dynamics simulations.[16]

Kilo et al. described experimental studies of lanthanide diffusion in YSZ and CSZ.[5] They use empirical potentials to calculate the energy landscape and to identify the lowest-energy diffusion path. They found that the path is nonlinear, with the saddle point located a significant distance from the midpoint of the linear path connecting a hopping cation and its target nearest neighbor vacancy site. They also reported activation enthalpies for a variety of lanthanides in YSZ and CSZ, along with Arrhenius prefactors.

In order to understand potential trade-offs between reducing thermal conductivity and degrading the mechanical performance of these materials, we have investigated the effect on cation diffusivity of the inclusion of substitutional Yb, Nb, and Gd in YSZ via kinetic Monte Carlo simulation. We discuss the dependence of cation diffusivity on doping species concentration, and on the presence of oxygen vacancies in the barrier complexes.

KINETIC MONTE CARLO METHOD

Kinetic Monte Carlo simulation differs from the more widely used Metropolis Monte Carlo method in that it is explicitly aimed at capturing the important features of "infrequent event" systems. While the first applications of the method date back to the 1960s, the method has enjoyed considerable recent popularity.[18-20]

Infrequent event systems are systems which evolve from state to state, but for which the system resides in a given state for a relatively long time, with infrequent and relatively rapid transitions between states. Diffusion is such a phenomenon; the state of the system is characterized by the location of all of its atoms, which typically reside in local energy minima located at lattice or interstitial points. Each atom undergoes thermal

vibrations, and, provided that the temperature is not too high, will only rarely escape from its local minimum and move to an adjacent vacant lattice or interstitial site. Further, because of the relatively large time an atom remains in the same minimum, it undergoes a large number of vibrations, and is effectively randomized, retaining no information about its location prior to its most recent hop.

The kMC method complements the more widely used molecular dynamics (MD) method. Provided that a system's dynamics can be accurately represented using classical or quantum-approximate potentials, MD simulations can produce a detailed trajectory for each particle in the simulation. However, accurately representing atomic vibrations in such simulations requires that the numerical integration of the equations of motion be carried out using a time step on the order of femtoseconds. This places a limit on the size of systems that may be effectively studied using MD, and on simulation duration as well.

This restriction means that MD can be very inefficient when used to study infrequent event systems, notably the diffusive hopping systems of interest here. In an MD simulation of a system containing only a small fraction of vacancies, a computational cell of reasonable size will experience a relatively small number of diffusive hops, with most of the computational resources spent computing the trajectories of atoms between the infrequent hops. By contrast, the kinetic Monte Carlo method allows one to concentrate on the events of interest, and to effectively consider only the average behavior of the system between such events, while giving up information on the detailed trajectories of all atoms in the simulation.

A diffusive hop typically takes place on a time scale much slower that the typical period of atomic vibration, so that the system effectively loses any memory of the details of the hop, i.e. which of the vacancy's neighbor atoms was involved in the most recent hop. Each such hop may therefore be considered to be an independent event. The probability per unit time that a vacancy will undergo a hop is constant, with the survival probability decreasing exponentially. The probability distribution *p(t)* of the time of first escape is given by $p(t) = k_{tot} \exp(-k_{tot} t)$, and the average time of first escape τ is given by $\tau = \int_0^\infty tp(t)dt = 1/k_{tot}$. Because all hopping events are independent, the effective total rate constant k_{tot} is just the sum of rate constants k_{AB} for all possible paths, with each rate constant determined by the height of the migration energy barrier in the direction of the hop:

$$k_{tot} = \sum_B k_{AB}$$

When the migration barrier energies are known, the hopping rates may be computed from $v_{AB} = v^0 \exp(-E_{AB}/k_B T)$ in which ν_{AB} and E_{AB} are the hopping rate and migration barrier energy for a hop between oxygen or cation sites A and B respectively, and ν^0 is the frequency factor. ν^0 is typically assigned a value between 10^{12} and 10^{13} for these materials; given that the measured diffusivities (both oxygen and cation) from different

studies can differ substantially, we assume a baseline value of 10^{13} with the understanding that the values of the diffusivities presented here involve considerable uncertainty. A species-specific correction to the frequency factor will be described later. For each possible hop, the hopping probability can be computed from the hopping rate, with $P_{AB} = \nu_{AB}/\Gamma$, where Γ is the sum of hopping rates for all possible hops in the computational cell. A catalog of all possible hops, and the corresponding hopping rates and probabilities, is created.

During the kMC process, one of the possible events (that is, a hop defined by the hopping ion and the target vacancy site) is chosen probabilistically from the catalog and executed. Hopping rates for all possible hops involving the new vacancy location are computed and added to the catalog, while rates involving the vacancy's previous location are deleted, and the sum of the hopping probabilities is updated. Finally, the simulation clock is advanced by a stochastically chosen time step $\Delta t = -\ln(R)/\Gamma$ where R is a random number greater than zero and less than or equal to unity.

When the simulation has run long enough to accumulate statistically useful information, the mean square displacement, averaged over all vacancies, is computed. The vacancy diffusivity D_v is obtained from the Einstein relation $\langle R^2 \rangle = 6 D_v t$, and the ionic diffusivity D_i is obtained by balancing the number of vacancy and ionic hops:

$$D_i = \frac{C_v}{1 - C_v} D_v$$

where C_v is the concentration of vacancies on the appropriate sublattice.

ENERGY BARRIERS

The most energetically favorable hopping path for cation diffusion is in the [110] direction, from a cation site to a nearest neighbor cation vacancy site, as confirmed by DFT calculations, and by the MD simulations of Kilo.[17]

Cation diffusivity is sensitive to the choice of migration barrier energy. However, the values of those quantities have not been definitively established. Solmon et al. report hopping enthalpies of 4.8-4.95eV in the range of 1300-1700°C.[21] Gomez-Garcia et al. report enthalpies of 5.5-6.0eV above 1500C.[22] Chien and Heuer[23] report a value of 5.3eV at 1100-1300°C, and Dimos and Kohlstedt[24] find a value of 5.85eV at 1400-1600°C. Kilo et al. find values of 4.4-4.8eV at 1125-1460°C.[15] Mackrodt et al. have calculated Y and Zr migration energies of 2-7eV for YSZ.[25]

A set of energy barriers has been calculated using density functional theory (DFT) as implemented in the Quantum Espresso code.[26] These barriers are in reasonable agreement with experiment, with the exception of the Zr barrier energy, which is about 35 percent too large. Kilo[17] presents activation enthalpies and Arrhenius prefactors D_0 for a variety of lanthanide dopants in YSZ, and we have used these data in our kMC simulations. These authors also reference barrier energies for Zr and Y, but more recent

work by these authors suggests different barrier energies for Zr and Y, and we have used these newer values in our work. The barrier energies and prefactors are shown in Table 1.

Table 1. Migration barrier energies and prefactors (D_0).

Species	Energy, eV	ln(D_0)
Zr	4.6	-2.3
Y	4.2	-3.7
Yb	4.9	0.01
Nd	4.7	-0.04
Gd	5.4	4.1

RESULTS AND DISCUSSION

Kilo et al. find that although the migration enthalpies are similar for a number of lanthanides, the diffusivities are different, which may be due to the substantially different Arrhenius prefactors. In order to incorporate these prefactors in the kMC methodology, we note the hopping probabilities are given by $\nu^0 = e^{(-E_a/k_bT)}$ and the inverse of the sum of the probabilities for all hopping vacancies in the simulation provides a time scale.

The baseline value for the vibrational frequency ν^0 is taken to be 10^{13}, as is commonly used in kMC simulations. This value has given reasonable agreement with experiment in the case of oxygen diffusion in YSZ.[3] Further, because neither the barrier energies nor the prefactors are very different between Y and Zr, assuming the same value for ν^0 is also reasonable for cation diffusion simulations of ZrO_2. However, while the lanthanide dopants considered here do have similar barrier energies, the prefactors vary by several orders of magnitude, and the assumption of a constant values for ν^0 for these materials is more problematic. We therefore assume that the values of ν^0 for all dopants, including Y, differ by the same factor as the ratios of the prefactors. All kMC runs were performed with these corrections to the vibrational frequencies.

Chien and Heuer obtained estimates of the concentrations of zirconium vacancies and cation-anion vacancy complexes.[23] Over a temperature range of 1100-1300°C, they estimated concentrations up to 10^{-8}. Kilo et al. extrapolated this data to temperatures above 3000°K and obtained concentrations up to 10^{-3}.[16] In this work we use a fixed concentration of 3×10^{-3}, not very different from the value of 4×10^{-3} used in the MD simulations of Kilo.

For most of the simulations described below it was assumed that the barrier complexes were fully populated, with no vacancies in the two-atom complex. In some cases, however, oxygen vacancies were assigned to the barrier complex sites stochastically, consistent with the concentration of cation dopants, as discussed below.

Arrhenius plots of kMC results for ZrO_2 and YSZ are presented in Figure 1, for a temperature range of 1000K to 3000K. The plots are close to identical, but there is a slight variation in the computed activation energies. This can be understood by noting

that the migration barrier energy for Y^{3+} is smaller than that of Zr^{4+}, so that increasing the concentration of yttria is expected to reduce the total activation energy and increase the diffusivity. The activation energy for ZrO_2 and YSZ with 4.55, 10 and 15 mol% yttria are 4.60eV, 4.504eV, 4.422eV and 4.364eV respectively, with the value for ZrO_2 reflecting the assumed activation energy for pure Zr diffusion.

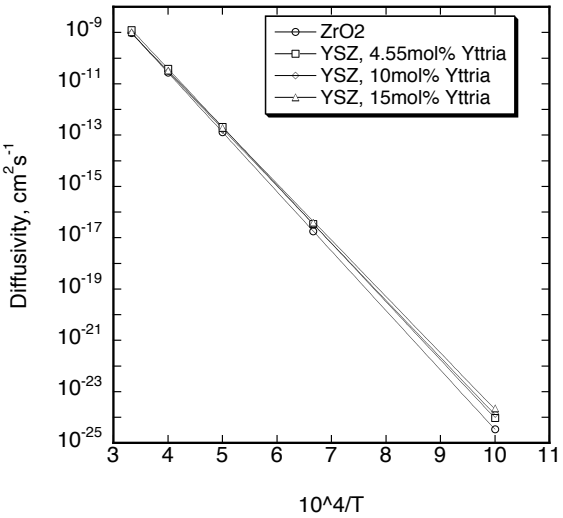

Figure 1. Temperature dependence of cation diffusivity in ZrO_2 and YSZ.

Figure 2 shows experimental results for YSZ, and some representative kMC results for YSZ 4.55 mol % Y_2O_3, and the same material additionally doped with 11.5 mol % Yb_2O_3 or 22.5 mol % Gd_2O_3. The kMC results are in good agreement with the experimental results of Kilo[16] and Chien[23], but agree less well with the results of Solmon.[21]

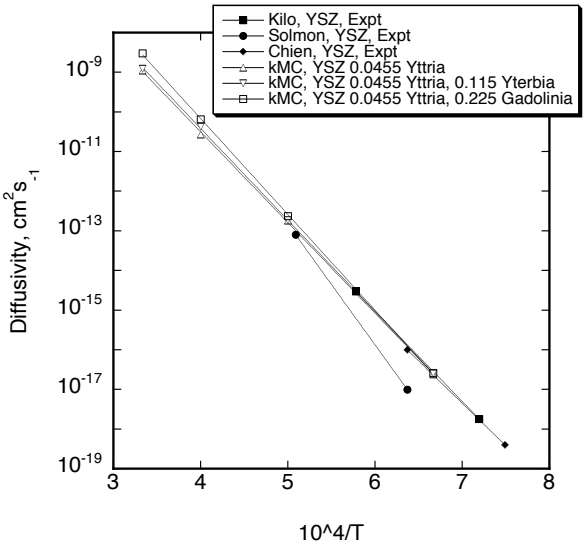

Figure 2. Comparison of experimental cation diffusivities with results from kinetic Monte Carlo simulations.

Arrhenius plots are shown in Figure 3 for the baseline YSZ/4.55 mol % Y_2O_3, and for the basline YSZ doped with Gd_2O_3, Nd_2O_3 or Yb_2O_3, at total dopant concentrations (including Y_2O_3) of 6 and 16 mol %. The greatest variation among the diffusivities is at the highest temperature, where the YSZ-Gd diffusivity is the largest, but by less than an order of magnitude.

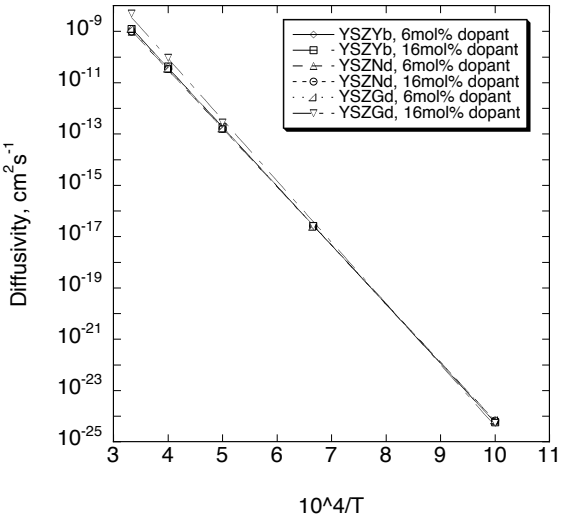

Figure 3. Diffusivities for YSZ doped with various aliovalent cations.

The concentration dependence of the diffusivity is shown in more detail in Figures 4a-b, where the diffusivities are plotted against dopant concentration, At 1500K there is no systematic concentration dependence, while at 3000K the diffusivity of YSZ-Gd diverges from that of the other two dopants, with the difference at 3000K being somewhat less than an order of magnitude.

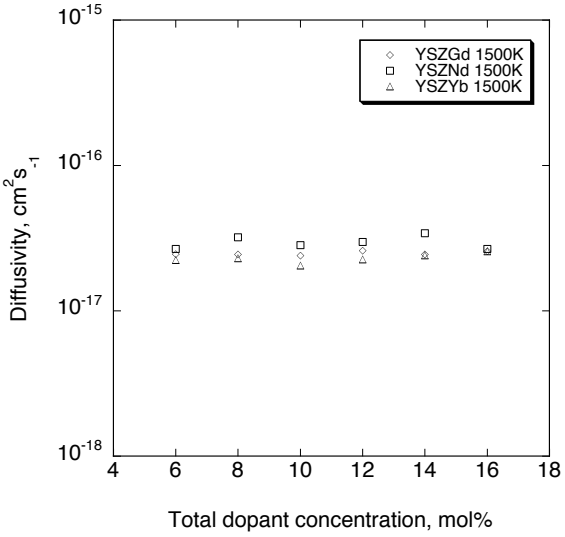

Figure 4a. Concentration dependence of diffusivities of doped YSZ. 1500°K.

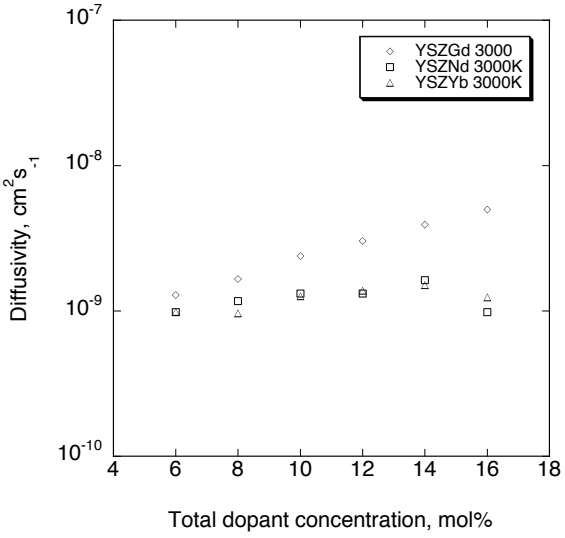

Figure 4b. Concentration dependence of diffusivities of doped YSZ. 3000°K.

The cation diffusivities of YSZ-Nd and YSZ-Yb are lower than that of YSZ-Gd at high temperature, suggesting that a YSZ-based material containing either of those dopants might be less susceptible to mechanical degradation than a material containing Gd, for degradation mechanisms, such as creep, that depend on the cation diffusivity. This conclusion is consistent with thermal cycling results on electron-beam physical-vapor-deposited coatings, but is not consistent with results from plasma-sprayed coatings.[6] The reason for this discrepancy is not yet clear, though there are pronounced differences between the microstructures in the two cases.

Finally, the effects of including oxygen vacancies in the barrier complexes are considered. We note that the concentration of oxygen vacancies depends on the concentration and charge state of the dopants. All the dopants considered here have a charge of +3, (compared with the Zr ions' charge of +4) so that a single oxygen vacancy is created for every pair of substitutional dopant cations. The concentration of these induced oxygen vacancies is much larger than the intrinsic concentration at the temperatures of interest here. The concentration of the dopant species therefore determines the fraction of barrier pairs on the oxygen sub lattice that include one or two oxygen vacancies.

DFT calculations of relaxed barrier energies for barriers containing a single oxygen were performed for Zr and Y, and the reductions in the barrier energies compared with the previously-calculated energies for fully-populated barriers. The ratios of the single- and double-atom barriers were used to scale the experimental energies shown in Table 1, with the result that the Zr and Y single-atom barrier energies were reduced to 1.776 and 1.717eV, respectively.

Results are shown in Figures5a-b. The plots were taken from kMC runs at 1500°K and 3000°K, for YSZ/4.55 mol % Y_2O_3, with and without barrier vacancies. At both temperatures, the diffusivity is larger when vacancies are included in the barriers. At 1500°K, both diffusivities increase with increasing yttria concentration. The diffusivity for the vacancy-containing material shows a much larger increase with concentration, with the difference between the two reaching a bit less than an order of magnitude at a yttria concentration of 20 mol %. At 3000°K, the diffusivity for YSZ without barrier vacancies is approximately independent of yttria concentration, while the vacancy-containing material increases by more than an order of magnitude.

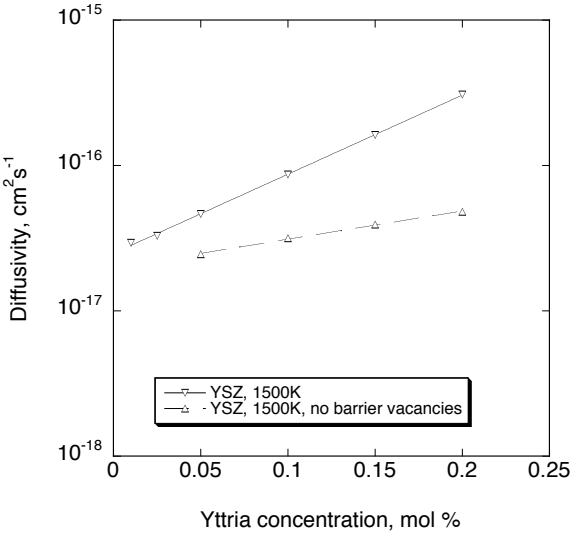

Figure 5a. Effect of vacancy-containing diffusion barriers on diffusivity of YSZ. 1500°K.

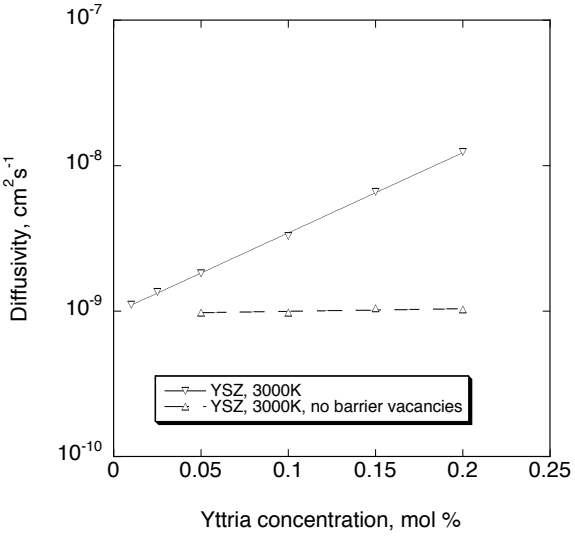

Figure 5b. Effect of vacancy-containing diffusion barriers on diffusivity of YSZ. 3000°K.

CONCLUSION

We have performed kinetic Monte Carlo computer simulations of cation diffusion in ZrO_2, undoped YSZ and YSZ doped with Gd, Nd and Yb. The kMC results for diffusivities and activation energies are in reasonable agreement with available experimental data. The activation energyy of YSZ is smaller than that of ZrO_2, and decreases with increasing yttria concentration. The diffusivity does not vary a great deal among the various dopants considered, with the largest diffusivity occurring in YSZ-Gd having a dopant concentration of 16 mol%, the largest dopant concentration investigated. Only YSZ-Gd shows a significant increase in diffusivity with dopant concentration.

The presence of an oxygen vacancy in the barrier complex reduces the migration barrier energy substantially, with the results that the diffusivity of YSZ is increased by as much as an order of magnitude at high yttria concentration. We expect similar behavior from the other dopants considered here.

The cation diffusivity of YSZ-Gd is somewhat larger than those of YSZ-Nd and YSZ-Yb. While this may indicate that YSZ-Gd is more likely to exhibit degradation via creep, the experimental evidence is ambiguous, and a more detailed understanding of the microstructures produced by different coating application methods is needed.

REFERENCES

[1]P. Aldebert and J. P. Traverse, J. Am Ceram. Soc. 68 [1], 34-40 (1985).
[2]R. E. W. Casselton, Phys. Status Solidi A, 2, 571-585 (1970).
[3]R. Krishnamurthy, Y.-G. Yoon, D. J. Srolovitz and R. Car, J. Am. Ceram. Soc. 87 1821-1830 (2004).
[4]R. Krishnamurthy, D. J. Srolovitz, K. N. Kudin and R. Car, J. Am. Ceram. Soc. 88 [8],2143-2151 (2005).
[5]M. Kilo, M.A. Taylor, Ch. Argirusis and G. Borchardt, B. Lesage, S. Weber, S. Scherrer, H. Scherrer, M. Schroeder and M. Martin, J. Appl. Phys. 94, 7547 (2003).
[6]D. Zhu and R. A. Miller, "Thermal Conductivity and Sintering Behavior of Advanced Thermal Barrier Coatings," NASA/TM-2002-211481
[7]P. K. Schelling, S. R. Phillpot and D Wolf, J. Am Ceram. Soc. 84 [7], 1609-1619 (2001).
[8]S. Fabris, A. T. Paxton and M. W. Finnis, Phys. Rev. B 63, 094101 (2001).
[9]M Fevre, A. Finel and R. Caudron, Phys. Rev. B 72, 104117 (2005).
[10]M Fevre, A. Finel, R. Caudron and R. Mevrel, Phys. Rev. B 72, 104118 (2005).
[11]M. S. Kahn, M. S. Islam and D. R. Bates, J. Mater. Chem. 8 [10], 2299-2307 1998.
[12]T. P. Perumal, V. Sridhar, K. P. N. Murthy, K. S. Easwarakumar and S. Ramasamy, Comp. Mat. Sci. 38, 865-872 (2007).
[13]F. Shimojo, T. Okabe, F. Tachibana, M. Kobayashi and H. Okazaki, J. Phys. Soc. Jpn 61, 2848-2857 (1992), and F. Shimojo and H. Okazaki, J. Phys. Soc. Jpn 61, 4106-4118 (1992).
[14]H. Okazaki, H. Suzuki and K. Ihata, Phys. Let. A 188, 291-295 (1994).
[15]M. Kilo, G. Borchardt, C. Lesage, O. Kaitsov, S. Weber and S. Scherer, J. Eur. Ceram. Soc., Faraday Trans. 5, 2069 (2000).
[16]M. Kilo, M. A. Taylor, C. Argirusis, G. Borchardt, R. A. Jackson, O Schulz, M. Martin and M. Weller, Solid State Ionics 175, 823-827 (2004).

[17]M. Kilo, M.A. Taylor, C. Argirusis, G. Borchardt, S. Weber, H. Scherrer and R.A. Jackson, J. Chem. Phys. 121, 5482 (2004).
[18]W. M. Young and E. W. Elcock, Proc. of the Phys. Soc. 89, 735 (1966) .
[19]A. B. Bortz and M. H. Kalos and J. L. Lebowitz, J. of Comput. Physics 17, 10 (1975).
[20]A. F. Voter, Kinetic Monte Carlo, in Radiation Effects in Solids, Proceedings of the NATO Advanced Study Institute on Radiation Effects in Solids, K. E. Sickafus, E. A. Kotomin, B. P. Uberuaga, eds., 1-23, Springer, Dordrecht, The Netherlands, 2007.
21H. Solmon, C. Monty, M. Filial, G. Petot-Ervas and C. Petot, Solid State Phenom. 41, 103 (1995).
[22]D. Gomez-Garcia, J. Martines-Fernandez, A. Dominguez-Rodriguez and J. Castaing, J. Am. Ceram. Soc. 80, 1668-1672 (1997).
[23]F. R. Chien and A. H. Heuer, Philos. Mag. A 73, 681-697 (1996).
[24]D. Dimos and D. L. Kohlstedt, J. Am. Ceram. Soc. 70, 277 (1987).
[25]W. C. Mackrodt and P. M. Woodrow, J. Am. Ceram. Soc. 68, 277 (1986).
[26]P. Giannozzi, S. Baroni, N. Bonini, M. Calandra, R. Car, C. Cavazzoni, D. Ceresoli, G. L. Chiarotti, M. Cococcioni, I. Dabo, A. Dal Corso, S. Fabris, G. Fratesi, S. de Gironcoli, R. Gebauer, U. Gerstmann, C. Gougoussis, A. Kokalj, M. Lazzeri, L. Martin-Samos, N. Marzari, F. Mauri, R. Mazzarello, S. Paolini, A. Pasquarello, L. Paulatto, C. Sbraccia, S. Scandolo, G. Sclauzero, A. P. Seitsonen, A. Smogunov, P. Umari, R. M. Wentzcovitch, J.Phys.:Condens.Matter, 21, 395502 (2009)